Available online at www.sciencedirect.com

SciVerse ScienceDirect

Ceramics International 39 (2013) 6453–6460

CERAMICS INTERNATIONAL

www.elsevier.com/locate/ceramint

Synthesis of Fe_2O_3 nanoparticles for nitrogen dioxide gas sensing applications

S.T. Navale[a], D.K. Bandgar[a], S.R. Nalage[a], G.D. Khuspe[a], M.A. Chougule[a], Y.D. Kolekar[b], Shashwati Sen[c], V.B. Patil[a,*]

[a]*Functional Materials Research Laboratory, School of Physical Sciences, Solapur University, Solapur 413255, India*
[b]*Department of Physics, University of Pune, Ganeshkhind, Pune 411006, India*
[c]*Crystal Technology Section, Technical Physics Division, BARC, Mumbai, India*

Received 21 November 2012; received in revised form 23 January 2013; accepted 23 January 2013
Available online 31 January 2013

Abstract

Iron (III) oxide, Fe_2O_3, nanoparticles of approximately 40 nm diameter were synthesized by sol–gel method and their nitrogen dioxide adsorption and desorption kinetics were investigated by custom fabricated gas sensor unit. The morphology and crystal structure of Fe_2O_3 nanoparticles were studied by scanning electron microscopy (SEM), field emission scanning electron microscopy (FESEM) and X-ray diffraction (XRD) respectively. The roughness of film surface was investigated by atomic force microscopy (AFM). Relative sensitivity of Fe_2O_3 nanoparticles for NO_2 sensor was determined by electrical resistance measurements. Our reproducible experimental results show that Fe_2O_3 nanoparticles have a great potential for nitrogen dioxide sensing applications operating at a temperature of 200 °C.

Keywords: Fe_2O_3 thin films; XRD; FESEM; Stability; NO_2 gas sensor

1. Introduction

Nitrogen dioxide, NO_2, is one of the highly toxic and most harmful gases emitted from combustion of the exhaust of automobile engines, home heaters, furnaces, plants, etc. [1]. It is a chemical asphyxiate, which affects on human's nervous system and could cause people to lose consciousness at a very low concentration. It's threshold limit value is 25 ppm and hence detection of NO_2 at a low concentration (10–200 ppm) is very crucial to protect human lives [2,3]. In the past, development of chemiresistive NO_2 sensor has been based on thin/thick films of metal-oxides such as SnO_2 [4], In_2O_3 [5], WO_3 [6], and NiO [7]. These metal oxides suffer from the inherent drawbacks of poor selectivity, long response time, limited detection range and requirement of a high operating temperature (>300 °C).

Nanostructured metal oxides with semiconducting properties are very attractive for fabricating low-cost chemical gas sensors with high sensitivity to hazardous gases. Extremely small grain size in such materials yields a very large surface area for contact between the metal oxide and a surrounding gaseous medium, thus high sensitivity is possible for exposure to various types of gases [8,9]. A key factor for semiconductor gas sensors is the possibility to make a use of nanoscale metal oxides with reproducible properties as regards structure, porosity, thickness, and grain size [10].

As an environment friendly n-type semiconductor, α-Fe_2O_3, has been proven to be a good gas sensitive material for detection of toxic, combustible, explosive and harmful gases in both domestic and industrial applications, extensive studies have been carried out to improve the gas sensing performances of the α-Fe_2O_3 based sensor [11,12]. It is well-known that the shape and size of α-Fe_2O_3 have a significant influence on its gas sensing properties [13–15].

In view of the importance of Fe_2O_3 for gas sensing applications, present paper demonstrates the fabrication of α-Fe_2O_3 thin film sensor on glass substrates using spin coating

*Corresponding author. Tel.: +91 21 72744770.
E-mail address: drvbpatil@gmail.com (V.B. Patil).

0272-8842/$ - see front matter © 2013 Elsevier Ltd and Techna Group S.r.l. All rights reserved.
http://dx.doi.org/10.1016/j.ceramint.2013.01.074

technique for detection of NO_2 at low concentration and lower operating temperature (< 300 °C). Attempts are made for the correlation between gas sensing properties and physical properties viz, morphology and structure of α-Fe_2O_3.

2. Experimental details

Nanostructured iron oxide thin films were deposited on glass substrate by using spin-coating method. X-ray diffraction (XRD) pattern of the film was taken for the phase identification and estimation of the average crystallite size using Philips PW-3710 model. The surface morphology of Fe_2O_3 thin films were observed through Field emission scanning electron spectroscopy, MIRA3 TESCAN model operating at 20 KV. Thickness of the film was measured by using AMBIOS make XP-1 surface profiler with vertical resolution 1 Å and thickness of the Fe_2O_3 film was in the range of 116–120 nm.

In order to measure the gas response, resistance of films was measured in ambient air and in gas atmosphere. For resistance measurements, two silver electrodes separated by 1 cm were deposited on Fe_2O_3 thin film and the resistance was measured using 6-digit Keithley 6514 Electrometer data acquisition system.

To monitor the gas response of Fe_2O_3 films to various gases, films were mounted inside a custom fabricated gas sensor unit. The schematic of gas sensor unit is shown in Fig. 1. The known gas NH_3, H_2S, Cl_2, C_2H_5-OH, and NO_2 of particular concentration was injected through a syringe at operating temperature of 200 °C. The schematic of Fe_2O_3 thin film gas sensor is shown in Fig. 2.

The electrical resistance of Fe_2O_3 film in air (R_a) and in the presence of NO_2 gas (R_g) was measured to find the gas

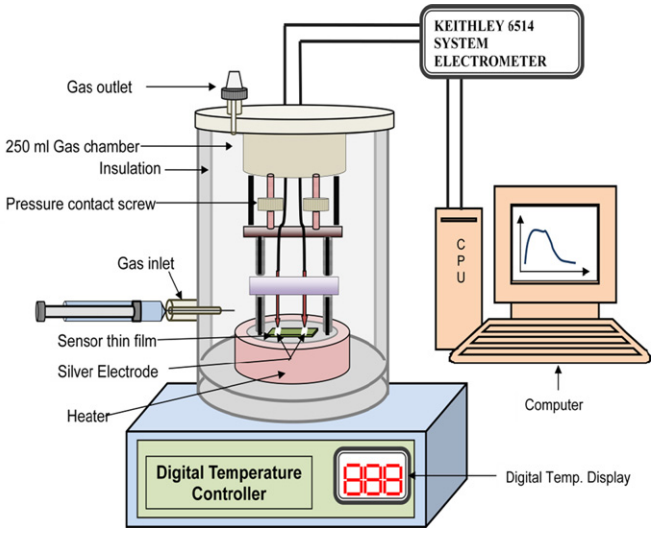

Fig. 1. Schematic of high temperature gas sensor unit.

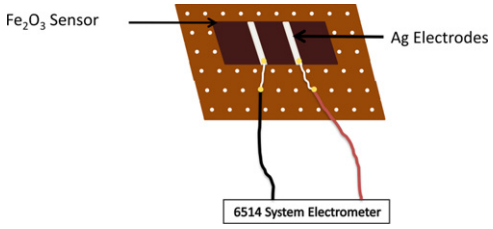

Fig. 2. Schematic of Fe_2O_3 thin film gas sensor.

response, S, defined as follows:

$$S(\%) = \frac{R_a - R_g}{R_a} \times 100\ \%$$

3. Results and discussion

3.1. Mechanism of Fe_2O_3 film formation

In a typical experiment; 3.315 g of iron chloride, $FeCl_3.6H_2O$, was added to 40 ml of methanol, CH_3-OH, and stirred vigorously at 60 °C for 1 h, leading to the formation of thick gel. Heating and stirring continuously further for 10 min, light green colored powder was obtained. As prepared powder was processed at various temperatures ranging from 400–700 °C with a fixed annealing time of 30 min in an ambient air to obtain nanocrystalline Fe_2O_3 with different crystallite sizes.

The possible chemical reaction mechanism of Fe_2O_3 nanocrystalline powder formation by novel chemical route is as follows:

1) $FeCl_3.6H_2O + 2CH_3\text{-}OH \underset{\text{Hydrolysis}}{\longleftrightarrow} CH_3O\text{-}Fe\text{-}OCH_3 + 2CH_3COOH + HCl + H_2O\uparrow$

2) $CH_3O\text{-}Fe\text{-}OCH_3 + H_2O \overset{\text{Alcohol Condensation}}{\underset{\text{Alcoholysis}}{\longleftrightarrow}} HO\text{-}Fe\text{-}OH + 2CH_3\text{-}OH\uparrow$

3) $HO\text{-}Fe\text{-}OH + HO\text{-}Fe\text{-}OH \overset{\text{Aging}}{\underset{\text{Polymerization}}{\longleftrightarrow}} OH\text{-}Fe\text{-}O\text{-}Fe\text{-}OH + H_2O\uparrow$

4) $OH\text{-}Fe\text{-}O\text{-}Fe\text{-}OH \overset{\text{Airannealing}}{\underset{\text{Oxidation}}{\longleftrightarrow}} Fe_2O_3 + 2H_2O\uparrow$

For sensor fabrication, the nanocrystalline Fe_2O_3 powder was further dissolved in m-cresol and continuously stirred for 1 h at room temperature for making casting solution. This casting solution was deposited on to a glass substrate by spin coating technique at 3000 rpm for 40 s and dried on hot plate at 100 °C for 10 min. The good electrical contacts were made with the silver paste strip of 1 mm wide and 1 cm apart from each other.

3.2. Structural analysis

Structural analysis of α-Fe_2O_3 films processed at 400–700 °C were carried out by using CuK_α radiation source of wavelength ($\lambda = 1.54056$ Å) and diffraction patterns of the films were recorded by varying diffraction angle (2θ) in the

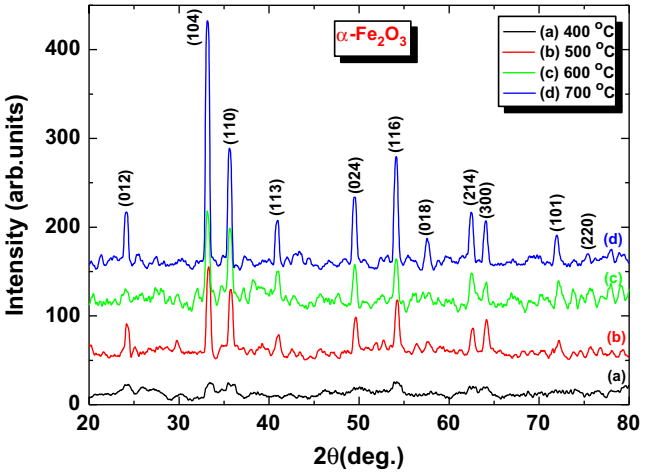

Fig.3. X-ray diffraction patterns of Fe_2O_3 film at different processing temperatures.

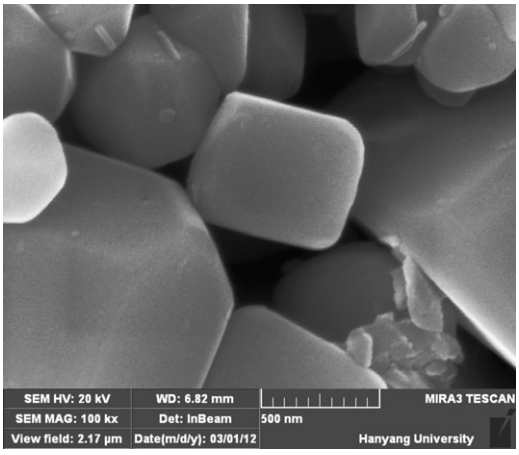

Fig.4. FESEM of Fe_2O_3 thin films processed at 700 °C.

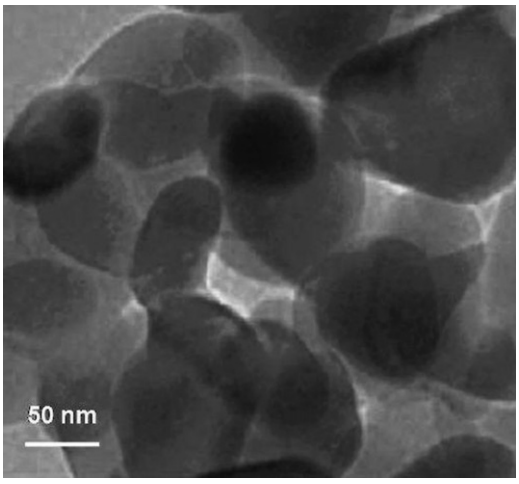

Fig. 5. TEM image of Fe_2O_3 processed at 700 °C.

range 20–80°. Fig. 3 shows the XRD pattern for Fe_2O_3 films processed at 400–700 °C. The diffraction peaks are indexed to the hexagonal phase of α-Fe_2O_3 with lattice parameters, $a=5.03$ Å and $c=13.74$ Å (JCPDS card no. 89–596) and the calculated 'd' values are in good agreement with the standard 'd' values. The well-defined diffraction peaks possesses orientations in the (012), (104), (110), (113), (024) (116), (018), (214), (300), (101) and (220) planes. The absence of any other impurity peaks suggests the purity of α-Fe_2O_3 formation. Further the broadening of peaks, compared with the bulk counterpart, indicates that the deposited material has a small crystallite size [16]. The average crystallite size of α-Fe_2O_3 was calculated by using Scherer's equation as

$$D = \frac{0.9\,\lambda}{\beta\cos\theta}$$

Where D is the average crystallite size, λ is wavelength of X-ray radiation ($\lambda=0.154$ nm), β is the full width at half maximum, and θ is the diffraction angle. It is observed that the average crystallite size was increased from 41 nm to 50 nm as the processing temperature increased from 400–700 °C.

As our earlier study [17] on α-Fe_2O_3 films processed between 400 and 700 °C showed that α-Fe_2O_3 film processed at 700 °C resulted into improved crystal structure, morphology, optical and electrical transport properties, therefore our further study in this paper aims at α-Fe_2O_3 film processed at 700 °C.

3.3. Field emission scanning electron microscopy (FESEM) analysis

Fig. 4 shows the field emission scanning electron micrograph (FESEM) of α-Fe_2O_3 films processed at 700 °C. From these micrographs, it is observed that the α-Fe_2O_3 film's surface is highly porous and consists of interconnected hexagonal grains, such morphology is preferred for gas sensing, as it promotes adsorption of gas molecules through the film surface [9].

3.4. Transmission electron microscopy (TEM) analysis

Microstructure of α-Fe_2O_3 film was observed by transmission electron microscopy and is shown in Fig. 5. TEM image of α-Fe_2O_3 nanoparticles showed the interconnected hexagonal nanoparticles with porous space in between them. Further, the micrographs indicate that the average particle size of α-Fe_2O_3 is in the 50–60 nm range.

3.5. Atomic force microscopy (AFM) analysis

The surface topography of α-Fe_2O_3 film processed at 700 °C was studied by atomic force microscopy in non contact mode. Fig. 6a and b shows the 2D and 3D AFM images (3 μm × 3 μm) of α-Fe_2O_3 nanoparticle film. From this figure, it is seen that the α-Fe_2O_3 film's surface is smooth and the surface morphologies of α-Fe_2O_3 nanoparticles confirms the hexagonal morphology evidenced by

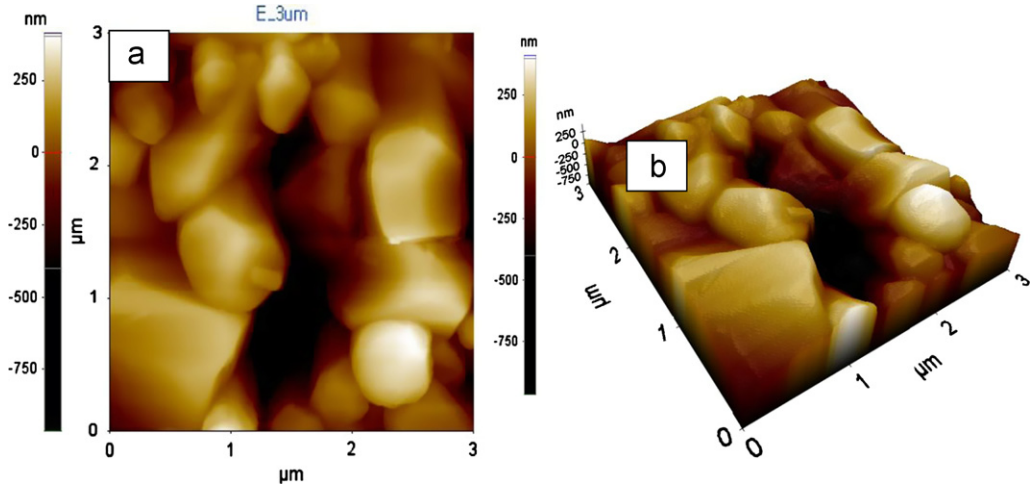

Fig. 6. AFM images of Fe_2O_3 thin films processed at 700 °C. (a) 2D image (b) 3D image.

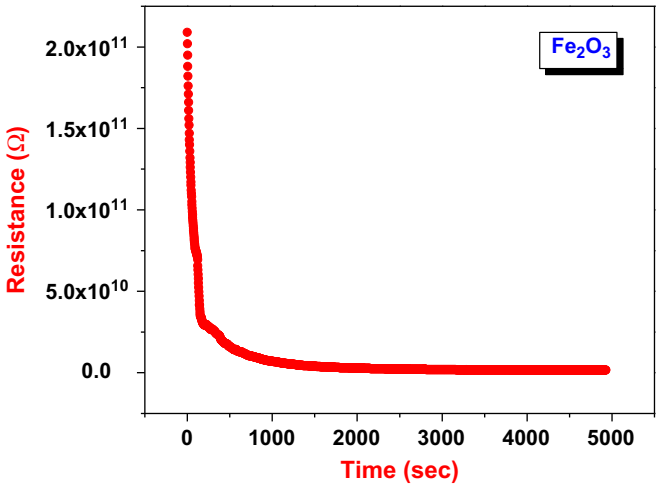

Fig.7. Resistance stabilization curve with time for Fe_2O_3 film at 200 °C.

FESEM and TEM micrographs. The surface roughness of the film over a 3μm × 3μm area was measured by AFM. The surface roughness mean square (RMS) of the film is 45 nm, which confirms that the surface morphology of α-Fe_2O_3 film processed at 700 °C is smooth.

3.6. Gas sensing properties

3.6.1. Stabilization of α-Fe_2O_3 sensor resistance

Stabilization of α-Fe_2O_3 film resistance in ambient air prior to exposure of gas is important because it ensures stable zero level for gas sensing applications. Since the TEM image of film processed at 700 °C showed the interconnected hexagonal nanoparticles with porous space in between them, it was decided to study the gas sensing properties of film processed at 700 °C. Fig. 7 shows the typical initial stabilization curve of the resistance of α-Fe_2O_3 film processed at 700 °C from nonequlibrium to equilibrium. Initially, when the temperature attained at 200 °C, the resistance was decreased rapidly within few seconds and then exhibited a stable value. This can be attributed to the generation of electrons due to thermal excitations. However, some of these electrons from the conduction band of α-Fe_2O_3 are extracted by oxygen adsorbed on the surface of the semiconductor, hence increasing the resistance of the semiconductor. The oxygen adsorbed undergoes the following reaction [18]

$$O_2(gas) \leftrightarrow O_2(ads) \quad (1)$$

$$O_2(ads) + e- \leftrightarrow O_2(ads) \quad (2)$$

$$O_2^-(ads) + e- \leftrightarrow 2O^-(ads) \quad (3)$$

Thus, the equilibration of chemisorptions process results in stabilization of surface resistance. Any process that disturbs this equilibrium gives rise to changes in the conductance of the semiconductors [18]. The conductance change is correlated with the concentration of gases in an ambient air.

3.6.2. Temperature dependent gas detection

Fig. 8 shows the bar diagram of gas response of different gases at fixed known concentration of 200 ppm of Fe_2O_3 film. The bar diagram showed that the sensor offered maximum response to NO_2 (17.16%) than H_2S, CH_3OH, C_2H_5-OH and NH_3. The sensor selects a particular gas at a particular temperature. Thus by setting the temperature, one can use the sensor for particular gas detection. The same sensor could be used for detection of different gases by operating at particular temperature for a typical gas. Different gases have different energies for adsorption, desorption and reaction on the metal oxide surface and therefore response of the sensor at different temperatures would depend on the gas being sensed. It is observed that the Fe_2O_3 film showed maximum response, at operating temperature of 200 °C, towards NO_2 as compared to H_2S, CH_3OH, C_2H_5-OH and NH_3 ($S_{NO2}/S_{H2S}=4.76$, $S_{NO2}/S_{CH3OH}=7.46$, $S_{NO2}/S_{C2H5OH}=12.26$ and $S_{NO2}/S_{NH3}=28.60$). It is revealed that Fe_2O_3 films were more selective towards NO_2 than other gases. Therefore, further dependence of NO_2 response on operating temperature and NO_2 concentration of Fe_2O_3 thin film was studied.

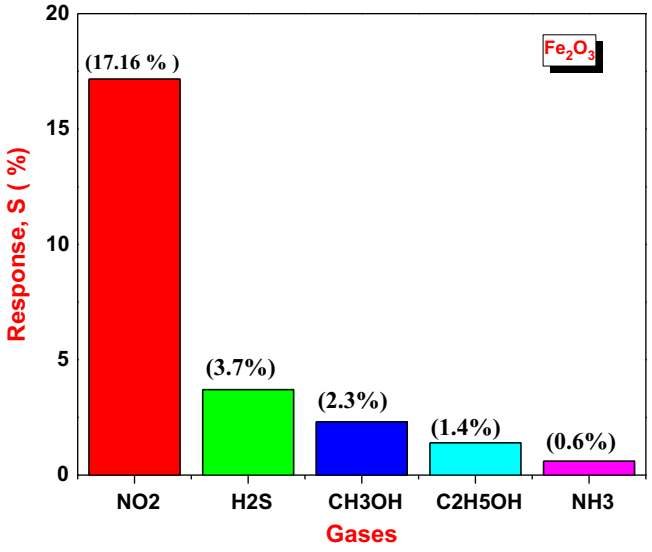

Fig.8. Gas response of Fe_2O_3 sensor to 200 ppm of NO_2, H_2S, CH_3OH, C_2H_5-OH and NH_3.

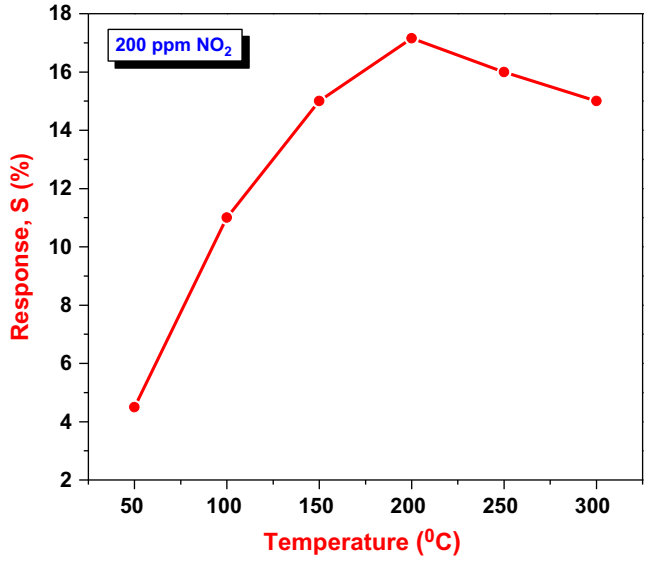

Fig. 9. Response of Fe_2O_3 films to 200 ppm of NO_2 gas as a function of operating temperature.

3.6.3. *Effect of operating temperature and NO_2 concentration:*

Before exposing to NO_2 gas, the Fe_2O_3 film was allowed to be stable for electrical resistance for 82 minutes and the stabilized resistance was taken as resistance in air (R_a). Initially, the gas response to 200 ppm of NO_2 was measured as a function of operating temperature for Fe_2O_3 film and is shown in Fig. 9. From this figure, it is seen that the Fe_2O_3 sensor response reached maximum at 200 °C (gas response = 17.16%) and then decreased. It is well known that at lower temperature, the response is restricted by the speed of chemical reaction, and at high temperature, by the speed of diffusion of gas molecules. At some intermediate temperature, the speeds of two processes become equal, and at that temperature, the sensor response reaches to its maximum [19].

3.6.4. *Gas sensing mechanism*

In case of n-type semiconductors, the electrons are injected into the conduction band recombine with some electrons and this process results an increase of the number of charge carriers, which leads to decreasing the resistance (opposite of p type) [20]. In our present study, similar behavior has been observed. However, electrical conductance of n-type semiconductors increases (or decreases) when reducing (or oxidizing) gases are adsorbed on their surface (opposite for p-type semiconductors) [21]. In all cases the sensors exhibited an increase in resistance upon exposure to the gases vapors and this suggests that the metal-oxide layers are behaving as expected for n-type semiconductors in response to an oxidizing gas. In an n-type semiconducting oxide, adsorbed oxygen behaves as a surface acceptor state, trapping holes from the valence band and hence increasing the electron concentration.

For Iron oxide thin film-based sensor elements, obtained by sol–gel spin coating method, the sensitivity (electrical resistivity) change in the NO_2 ambient can be caused by the change in surface composition of the oxide layer at the chemisorption of gas molecules. The mechanism of nitrogen dioxide detection of tested sensors at 200 °C operating temperature can be explained by the chemisorption and removal of the surface chemisorbed species.

The desorption of NO_2^-(ad) is limited at the decomposition of NO_2 at the iron oxide, which is determined by the extensive recovery time after the expose of sensor to highly toxic NO_2 gas and depend on the sensors operating temperature as can be concluded from Fig. 9. At a higher operating temperature (~200 °C) the increase in response for samples can be explained by reversible oxidizing interaction of NO_2 molecules with sufficient thermal energy with the predominant surface adsorbed oxygen species

$$O_2^- \rightarrow 2O^- + e^- \quad (4)$$

Physisorbed nitrogen dioxide molecules form new surface acceptor levels deeper than the surface oxygen ions. Therefore, bound electrons are transferred from O_2^- ion to physisorbed NO_2 molecules

$$NO_2 + e^- \rightarrow NO_2^-(ad) \quad (5)$$

and form NO_2^- species and increased band bending at the iron oxide surface [22,23]. This can be explained the resistivity increase when sensor is placed in a test atmosphere. According to performed investigations, the NO_2 gas adsorption is principally a function of surface properties and requires a further research.

Once the operating temperature is fixed, the sensor response is studied at different NO_2 concentrations. Fig. 10 shows the response of Fe_2O_3 film as a function of NO_2 concentration. The response increased from 2.07 to 17.6%, as the NO_2 concentration increased from 10 to 200 ppm. The gas response showed saturation at more

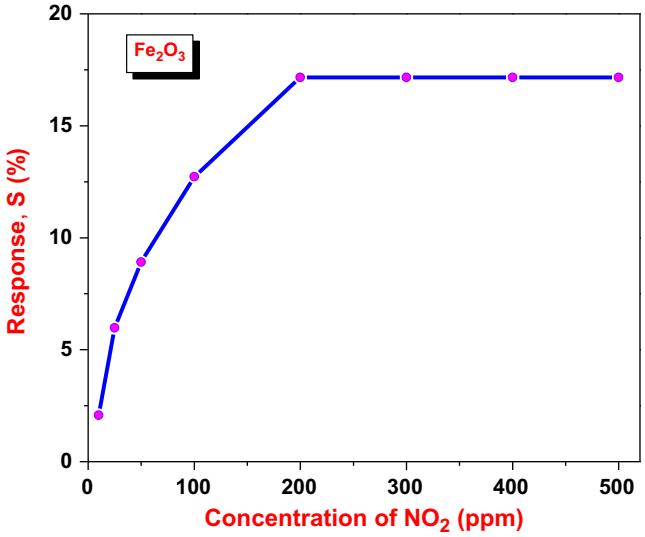

Fig. 10. Variation of NO_2 response of Fe_2O_3 film with different concentration of NO_2.

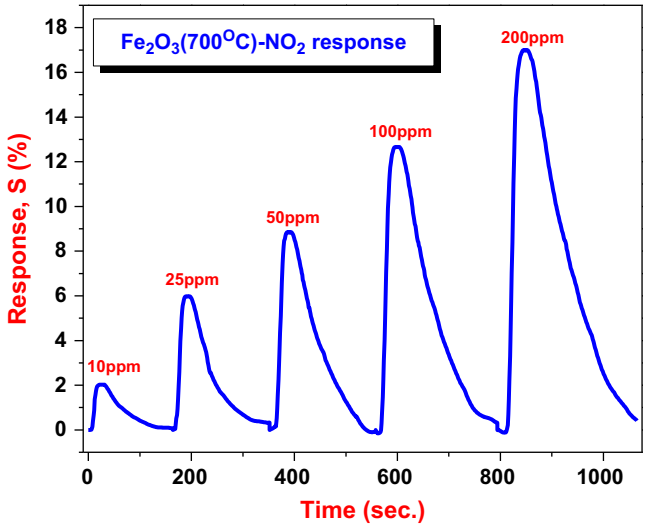

Fig. 11. Dynamic response of Fe_2O_3 thin film for 10–200 ppm of NO_2.

than 200 ppm concentration of NO_2, due to increased surface reaction [24,25]. The response of a sensor depends on the removal of adsorbed oxygen molecules by reaction with a target gas and generation of electrons. For a small concentration of gas, exposed to a fixed surface area of a sample, there is a lower coverage of gas molecules on the surface and hence lower surface reactions are occurred. An increase in gas concentration increases the surface reaction due to larger surface coverage. A further increase in surface reaction will be gradual when the saturation point on the coverage of molecules is reached [26].

3.6.5. *Dynamic response transients of Fe_2O_3 thin films*

The dynamic variation of response of the iron oxide thin film with time upon exposure to 20–200 ppm of NO_2 at 200 °C is shown in Fig. 11. From this Fig. 11, it is observed that the response increased from 2.07 to 17.16% with increasing the gas concentration of NO_2 from 10 to 200 ppm. At 200 ppm, the Fe_2O_3 film showed the maximum response of 17.16%. Such a maximum response is due to interactions between the NO_2 gas and the surface of Fe_2O_3 film. So, it is obvious that for the materials of greater surface area, the interactions between adsorbed gases and sensor surface are significant [27].

3.6.6. *Response and recovery time of Fe_2O_3 films*

The response/recovery time is an important parameter used for characterizing a sensor. The response time is defined as the time at which the resistance of iron oxide thin film reaches to 90% of the saturation value on exposure to NO_2 and the recovery time is defined as the time required for recovering the 90% of the original resistance [28,29]. The variation of response and recovery time with different concentrations of NO_2 at operating temperature 200 °C is shown in Fig. 12. It is observed that the response time decreased from 20 to 12 seconds while

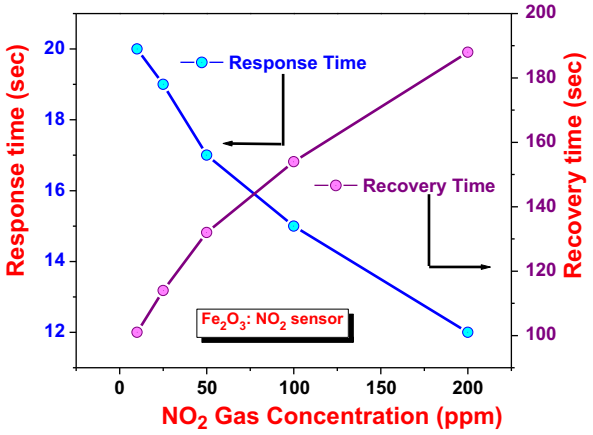

Fig.12. Variation of response and recovery time of Fe_2O_3 with NO_2 concentration.

recovery time increased from 101 to 188 seconds as the NO_2 concentration increased from 10 to 200 ppm. The decrease in response time may be due to large availability of vacant sites on the film for gas adsorption as evident from FESEM image and increase in the recovery time may be due to the heavier nature of NO_2 and the reaction products are not leaving from the interface immediately after the reaction resulting in decrease in desorption rate Fig. 13.

3.6.7. *Reproducibility and stability of Fe_2O_3 thin film sensor*

The sensor reliability is strongly dependent on the reproducibility and stability exhibited by the sensor material. The reproducibility of the Fe_2O_3 thin film NO_2 sensor for 200 ppm operating at 200 °C was measured by repeating the response measurement a number of times. It is observed that the response of Fe_2O_3 sensor towards NO_2 at 200 ppm is almost constant (Response value is 17.12%) confirming the reproducibility of sensor material. In order to measure the stability of Fe_2O_3 thin film sensor, response

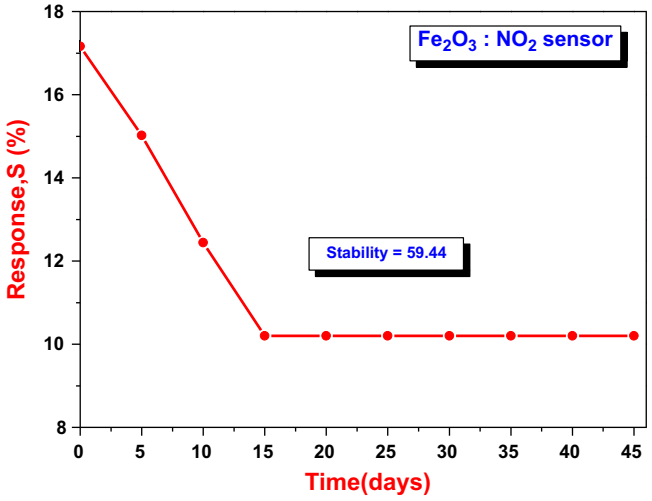

Fig.13. Stability of Fe_2O_3 thin film at operating temperature of 200 °C.

of the sensor was tested at fixed temperature (200 °C) and concentration of NO_2 (200 ppm) for 45 days at an interval of 5 days. Initially Fe_2O_3 sensor shows relatively maximum response, however it was dropped from 17.16% to 10.2% and stable response was obtained after 15 days with 59.44% stability. This is because in the initial stage Fe_2O_3 sensor may undergo interface modification during operation and then reaches to steady state indicating the stability of Fe_2O_3 sensor operating at 200 °C temperature.

4. Conclusion

Nanostructured α-Fe_2O_3 thin film sensor was fabricated on glass substrate by low cost sol–gel spin coating technique. Structural analysis showed formation of hexagonal α-Fe_2O_3. Microstructural analysis confirms nanostructured morphology suitable for gas sensing applications. The gas sensing measurements at 200 °C showed that α-Fe_2O_3 films are selective to NO_2 gas and exhibits maximum response of 17.12% with 59.44% stability. The gas sensing properties viz, selectivity, response and stability showed that α-Fe_2O_3 would be a potential candidate for NO_2 gas sensor.

Acknowledgments

Authors are grateful to the Department of Atomic Energy-Board of Research in Nuclear Science, Govt. of India, New Delhi for financial support through the scheme no. 2010/37 P/45/BRNS/1442.

References

[1] Y. Shimizu, M. Egashira, Basic aspects and challenges of semiconductor gas sensors, MRS Bulletin (1999) 18–24.
[2] V.E. Bochenkov, G.B. Sergeev, Preparation and chemiresistive properties of nanostructured materials, Advances in Colloid and Interface Science 116 (2005) 245–254.
[3] G. Martinelli, M.C. Carotta, M. Ferroni, Y. Sadaoka, E. Traversa, Screen printed perovskite-type thick films as gas sensors for environmental monitoring, Sensors and Actuators B 55 (1999) 99.
[4] M. Law, H. Kind, B. Messer, F. Kim, P.D. Yang, Photochemical sensing of NO_2 with SnO_2 nanoribbon nanosensors at room temperature, Angewandte Chemie International Edition 41 (2002) 2405–2408.
[5] D. Zhang, Z. Liu, C. Li, T. Tang, X. Liu, S. Han, B. Lei, C. Zhou, Detection of NO_2 down to ppb levels using individual and multiple In_2O_3 nanowire devices, Nano Letters 4 (2004) 1919–1924.
[6] W. Noh, Y. Shin, Effects of NiO addition in WO_3-based gas sensors prepared by thick film process, Solid State Ionics 152 (2002) 827–832.
[7] I. Hotovy, V. Rehacek, P. Siciliano, S. Capone, L. Spiess, Sensing characteristics of NiO thin films as NO2 gas sensor, Thin Solid Films 418 (2002) 9–15.
[8] S.R. Nalage, M.A. Chougule, Shashwati Sen, V.B. Patil, Fabrication and characterization of nickel oxide NO_2 sensor, Journal of Materials Science: Materials in Electronics 24 (2013) 368–375.
[9] M.A. Chougule, Shashwati Sen, V.B. Patil, Fabrication of nanostructured ZnO thin film sensor for NO_2 monitoring, Ceramics International 38 (2012) 2685–2692.
[10] S.G. Pawar, S.L. Patil, M.A. Chougule, B.T. Raut, S.A. Pawar, R.N. Mulik, V.B. Patil, Nanocrystalline TiO_2 thin films for NH_3 monitoring: microstructural and physical characterization, Journal of Materials Science: Materials in Electronics 23 (2012) 273–279.
[11] S. Wang, L. iWang, T. Yang, X. Liu, J. Zhang, B. Zhu, S. Zhang, W. Huang, S. Wu, Porous α-Fe_2O_3 hollow micro spheres and their application for acetone sensor, Journal of Solid State Chemistry 183 (2010) 2869–2876.
[12] L. Huo, Q. Li, H. Zhao, L. Yu, S. Gao, J. Zhao, Sol–gel route to pseudo cubic shaped α-Fe_2O_3 alcohol sensor: preparation and characterization, Sensors and Actuators B 107 (2005) 915–920.
[13] S.Y. Wang, W. Wang, W.Z. Wang, Z. Jiao, J.H. Liu, Y.T. Qian, Characterization and gas-sensing properties of nanocrystalline iron (III)oxide films prepared by ultrasonic spray pyrolysis on silicon, Sensors and Actuators B 69 (2000) 22–27.
[14] E.T. Lee, G.E. Jang, C.K. Kim, D.H. Yoon, Fabrication and gas sensing properties of α-Fe_2O_3 thin film prepared by plasma enhanced chemical vapor deposition (PECVD), Sensors and Actuators B 77 (2001) 221–227.
[15] Q. Hao, L. Li, X. Yin, S. Liu, Q. Li, T. Wang, Anomalous conductivity-type transition sensing behaviors of n-type porous α-Fe_2O_3 nanostructures toward H_2S, Materials Science and Engineering B 176 (2011) 600–605.
[16] E. Comini, G. Faglia, G. Sberveglieri, Z. Pan, Z.L. Wang, Stable and highly sensitive gas sensors based on semiconducting oxide nanobelts, Applied Physics Letters 81 (2002) 1869–1871.
[17] S.T. Navale, D.K. Bandgar,S.R. Nalge,R.N. Mulik, S.A. Pawar, M.A. Chougule, V.B. Patil, Journal of Materials Science: Materials of Electronics, 10.1007/s10854-012-0944-x,.
[18] K. Arshak, I. Gaidan, Development of a novel gas sensor based on oxide thick films, Materials Science and Engineering B. 118 (2005) 44–49.
[19] N.J. Dayan, S.R. Sainkar, R.N. Karekar, R.C. Aiyer, Formulation and characterization of ZnO: Sb thick-film gas sensors, Thin Solid Films 325 (1998) 254–258.
[20] S.L. Patil, S.G. Pawar, A.T. Mane, M.A. Chougule, V.B. Patil, Nanocrystalline ZnO thin films: optoelectronic and gas sensing properties, Journal of Materials Science: Materials of Electronics 21 (2010) 1332–1336.
[21] M. Mabrook, P. Hawkins, A rapidly-responding sensor for benzene, methanol and ethanol vapours based on films of titanium dioxide dispersed in a polymer operating at room temperature, Sensors and Actuators B, Chemical 75 (2001) 197–202.
[22] G. Martinelli, M.C. Carotta, M. Ferroni, Y. Sadaoka, E. Traversa, Screen-printed perovskite-type thick films as gas sensors for environmental monitoring, Sensors and Actuators, B, Chemical 55 (1999) 99–110.
[23] M. Law, H. Kind, B. Messer, F. Kim, P.D. Yang, Photochemical sensing of NO_2 with SnO_2 nanoribbon nano sensors at room temperature, Angewandte Chemie International Edition 41 (2002) 2405–2408.

[24] M.S. Tong, G.R. Dai, D.S. Gao, Surface modification of oxide thin film and its gas-sensing properties, Applied Surface Science 171 (2001) 226–230.
[25] S. Saito, M. Miyayama, K. Kaumoto, H. Yanagida, Gas Sensing Characteristics of Porous ZnO and Pt/ZnO Ceramics, Journal of the American Ceramic Society 68 (1985) 40–43.
[26] E. Traversa, New ceramic materials for chemical sensors, Journal of Intelligent Materials Systems Structures 6 (1995) 860–869.
[27] S.G. Pawar, S.L. Patil, M.A. Chougule, B.T. Raut, S.A. Pawar, R.N. Mulik, V.B. Patil, Nanocrystalline TiO_2 thin films for NH_3 monitoring: microstructural and physical characterization, Journal of Materials Science: Materials in Electronics 23 (2012) 273–279.
[28] G. Korotcenkov, V. Brinzari, J. Schwank, M. DiBattista, A. Vasiliev, Peculiarities of SnO_2 thin film deposition by spray pyrolysis for gas sensor application, Sensors and Actuators B 77 (2001) 244–252.
[29] B.T. Raut, P.R. Godse, S.G. Pawar, M.A. Chougule, .B. Patil, Development of nanostructured CdS sensor for H_2S recognition: structural and physical characterization, Journal of Materials Science: Materials in Electronics 23 (2012) 956–963.